

Exact General Relativistic Disks with Magnetic Fields

*Patricio S. Letelier*¹

Departamento de Matemática Aplicada-IMECC
Universidade Estadual de Campinas, 13083-970 Campinas. S.P., Brazil

Abstract

The well-known “displace, cut, and reflect” method used to generate cold disks from given solutions of Einstein equations is extended to solutions of Einstein-Maxwell equations. Four exact solutions of the these last equations are used to construct models of hot disks with surface density, azimuthal pressure, and azimuthal current. The solutions are closely related to Kerr, Taub-NUT, Lynden-Bell-Pinault and to a one-soliton solution. We find that the presence of the magnetic field can change in a nontrivial way the different properties of the disks. In particular, the pure general relativistic instability studied by Bičák, Lynden-Bell and Katz [Phys. Rev. D47, 4334, 1993] can be enhanced or cured by different distributions of currents inside the disk. These currents, outside the disk, generate a variety of axial symmetric magnetic fields. As far as we know these are the first models of hot disks studied in the context of general relativity.

PACS numbers: 04.20.Jb, 04.40.Nr, 98.62.En.

¹e-mail: letelier@ime.unicamp.br

1 Introduction

The existent magnetic fields in the primeval cloud of plasma that originates stellar objects like galaxies and stars remain after the formation of the objects. The magnetic lines of force are said to be “frozen in” the fluid. This field can play many different roles in astrophysics. Two examples are: The radius of a white dwarf for extreme relativistic degeneracy can change significantly even when a small quantity of magnetic energy is present [1]. Binary and active-galactic-nuclei disks are hot enough to be significantly or fully ionized, and their high conductivity allows the current to flow freely. The presence of magnetic fields strongly influence the structure and evolution of these disks [2].

Axially symmetric solutions of Einstein field equations corresponding to disk like configurations of matter are of great astrophysical interest and have been extensively studied. These solutions can be static or stationary and with or without radial pressure. Solutions for static disks without radial pressure were first studied by Bonnor and Sackfield [3], and Morgan and Morgan [4], and with radial pressure by Morgan and Morgan [5], and, in connection with gravitational collapse, by Chamorro, Gregory and Stewart [6]. Disks with radial tension has been recently considered in [7].

The stability of models with no radial pressure can be explained by either assuming the existence of hoop stresses or that the particles on the disk plane move under the action of their own gravitational field in such a way that as many particles move clockwise as counterclockwise. This last interpretation is frequently made since it can be invoked to mimic true rotational effects. A large class of thin disks solutions were obtained by Letelier and Oliveira [8]. Solutions for self-similar static disks were analyzed by Lynden-Bell and Pineault [9], and Lemos [10]. The superposition of static disks with black holes were considered by Lemos and Letelier [11, 12, 13], and Klein [14]. Recently Bičák, Lynden-Bell and Katz [15] studied static disks as sources of known vacuum spacetimes and Bičák, Lynden-Bell and Pichon [16] found an infinity number of new static solutions.

The above mentioned solutions of the Einstein equations have no sources other than the disk itself, i.e., outside the disk their metrics are solutions of the vacuum Einstein equations for static spacetimes with axial symmetry. The search of new solutions is facilitated in this case by the fact that one of the Einstein equations is equivalent to the usual (linear) Laplace equation.

In the present paper we study models of disks that are characterized by a surface density, an azimuthal pressure and a *current density*. Out side the disk the metric satisfy the Einstein-Maxwell equations for a static axially

symmetric spacetime filled with a magnetic field. As far as we know these are the first models of hot disks studied in the context of general relativity.

We find that the presence of the magnetic field can change in a nontrivial way the different properties of the disks. In particular, the pure general relativistic instability studied by Bičák, Lynden-Bell and Katz [15] can be enhanced or cured by different distributions of currents that outside the disk generate magnetic fields of different forms.

In Sec. II we study the Einstein-Maxwell equations for a static axially symmetric spacetime. We introduce the well known “displace, cut, and reflect” method to generate a disk from a given solution of these equations. We also present the expressions for the main physical variables of the disk. In the next section, Sec. III, four models of disks are studied. They are based in simple solutions to the Einstein-Maxwell equations. The first two are similar to Kerr and Taub-NUT solutions. The third is a generalization of a Lynden-Bell and Pinault solution [9] and the last is one obtained using solitonic techniques [17]. In the last section, Sec. IV, we discuss some of the found results and make some comments.

2 Einstein-Maxwell Equations and Disks

The simplest metric to describe static and axially symmetric systems is the Weyl metric,

$$ds^2 = f dt^2 - f^{-1} [e^w (dz^2 + dr^2) + r^2 d\varphi^2], \quad (1)$$

where the functions f and w depend only on the cylindrical coordinates r and z .

The Einstein-Maxwell system of equations is equivalent with,

$$G^{\mu\nu} = -T^{\mu\nu}, \quad (2)$$

$$T^{\mu\nu} = F^\mu{}_\alpha F^{\alpha\nu} - \frac{1}{4} g^{\mu\nu} F^{\alpha\beta} F_{\alpha\beta}, \quad (3)$$

$$\nabla_\alpha F^{\alpha\mu} = 0, \quad (4)$$

$$F_{\mu\nu} = \partial_\mu A_\nu - \partial_\nu A_\mu, \quad (5)$$

where all the symbols have their usual meaning. Now we choose the magnetic potential as

$$A_\mu = A(r, z) \delta_\mu^\varphi, \quad (6)$$

in other words we take the electromagnetic potential for a pure axially symmetric magnetic field,

$$F_{\varphi z} = -\partial_z A, \quad F_{r\varphi} = \partial_r A. \quad (7)$$

Therefore the physical components of the magnetic field are,

$$B_{\hat{r}} = -(f/r)e^{-w/2}\partial_z A, \quad (8)$$

$$B_{\hat{z}} = (f/r)e^{-w/2}\partial_r A. \quad (9)$$

From (1)–(4) we find the well known system of Einstein-Maxwell equations for axially symmetric spacetimes with pure magnetic fields [18],

$$\partial_r w = \frac{r[(\partial_r f)^2 - (\partial_z f)^2]}{2f^2} + \frac{f[(\partial_r A)^2 - (\partial_z A)^2]}{r}, \quad (10)$$

$$\partial_z w = \frac{r\partial_r f\partial_z f}{f^2} + \frac{2f\partial_r A\partial_z A}{r}, \quad (11)$$

$$\partial_r(r\partial_r f/f - fA\partial_r A/r) + \partial_z(r\partial_z f/f - fA\partial_z A/r) = 0, \quad (12)$$

$$\partial_r(f\partial_r A/r) + \partial_z(f\partial_z A/r) = 0. \quad (13)$$

Once the solution of the system of equations (12)–(13) is known, Eqs. (10)–(11) give us the function w as a quadrature whose existence is guaranteed by the previous equations.

The method that we shall use to generate the metric of the disk, as well as, its material and electromagnetic content will be the well known “displace, cut and reflect” method that was first used in Newtonian gravity by Kusmin [19] and Toomre [20] and later in general relativity by most of the authors that write about disks and also fine shells, defects, etc.

The material content of the disk will be described by functions that are distributions with support on the disk. The method that we shall use can be divided in the following steps: First, choose a surface that divide the usual space in two parts; one with no singularities or sources and the other with the sources. Second, disregard the part of the space with singularities. Third, use the surface to make an inversion of the nonsingular part of the space. The result will be a space with a singularity that is a delta function with support on the surface. This procedure is depicted in Fig. 1 for the gravitational field of a punctual mass.

In the present case the procedure is equivalent to make the transformation $z \rightarrow z_0 + |z|$, with z_0 constant. In the Einstein equation for axial symmetry we have first and second derivatives of z . Note that $\partial_z |z| = 2\theta(z) - 1$

and $\partial_z \theta(z) = \delta(z)$ where $\theta(z)$ is the Heaveside function and $\delta(z)$ the usual Dirac distribution.

The procedure above mentioned applied to the metric (1) and then Einstein-Maxwell equations gives us

$$G_{\mu\nu} = -(T_{\mu\nu}^{elm} + \hat{T}_{\mu\nu}), \quad (14)$$

$$\nabla_\mu F^{\mu\nu} = \hat{J}^\nu, \quad (15)$$

with

$$\hat{T}_0^0 = \rho = e^{-w}(2\partial_z f - f\partial_z w)\delta(z), \quad (16)$$

$$\hat{T}_\varphi^\varphi = P_\varphi = e^{-w}f\partial_z w\delta(z), \quad (17)$$

$$\hat{J}^\varphi = 2f\partial_z A\delta(z)/r, \quad (18)$$

where $\partial_z f$ should be understood as $\partial_z f|_{z=0+}$, etc. $T_{\mu\nu}^{elm}$ is the electromagnetic energy-momentum tensor defined in (3), $\hat{T}_{\mu\nu}$ is the matter energy-momentum tensor on the plane $z = 0$ and \hat{J}^μ is the current density on the plane $z = 0$. The ‘‘physical measure’’ of length in the direction ∂_z for the metric (1) is $(e^w/f)^{1/2}dz$, then the invariant distribution is $\delta(z)/(e^w/f)^{1/2}$. Therefore the surface density and the planar pressure or tension along the direction ∂_φ are,

$$\sigma = [(e^{-w}/f)^{1/2}(2\partial_z f - f\partial_z w)]_{z=0+}, \quad (19)$$

$$p_\varphi = [(fe^{-w})^{1/2}\partial_z w]_{z=0+}. \quad (20)$$

In the same form one can compute the tetradical component of the planar current density, we find,

$$j_\varphi = 2[e^{w/2}\partial_z A]_{z=0+}. \quad (21)$$

Another physically meaningful quantity associated to non rotating disks is the counter-rotation velocity,

$$V^2 = p_\varphi/\sigma = \frac{f\partial_z w}{2\partial_z f - f\partial_z w}\Big|_{z=0+}. \quad (22)$$

The disk is supposed to be formed by the same number of particles moving in circles in one direction than in the opposite direction. The specific angular-momentum of a particle with rest mass μ rotating at a radius r , defined as $h = \pi_\varphi/\mu = g_{\varphi\varphi}d\varphi/ds$, is

$$h = \frac{r\sqrt{p_\varphi\sigma}}{f\sqrt{\sigma^2 - p_\varphi^2}}. \quad (23)$$

This last quantity can be used to detect instability of the disk against radial perturbations (ring formation). The condition of stability is usually presented as

$$\frac{d(h^2)}{dr} > 0, \quad (24)$$

i.e, for $h > 0$ we have stability when the specific angular momentum is an increasing function of r for $0 < r < R$ (R the radius of the disk). This criteria is an extension of Rayleigh criteria of stability of a fluid at rest in a gravitational field, see for instance [21]. For other significant quantities for relativistic disks see [15].

As we said before in the present case the spacetime is static, hence in the disk we do not have a net movement of matter in one direction, but we have current along the ∂_φ direction. This means that we have a kind of moving massless charge approximation.

The field lines of the magnetic field are given by the ordinary differential equation,

$$\frac{dz}{B_z} = \frac{dr}{B_r}. \quad (25)$$

From (8) and (9) we find,

$$\partial_r A dr + \partial_z A dz = 0. \quad (26)$$

Thus the equation $A(r, z) = C$ (C constant) gives as the lines of force of the magnetic field.

3 Exact Disks with Magnetic Fields

There are many techniques to find exact solutions of (12)–(13), they are based in the fact that this system of equations has extra symmetries (Geroch group [22]) and that is closely related to the principal sigma model [17]. In particular, we can write (12)–(13) in the matrix form

$$\partial_r[r\partial_r(M)M^{-1}] + \partial_z[r\partial_z(M)M^{-1}] = 0, \quad (27)$$

where

$$M = \begin{pmatrix} f^{1/2} & (f/2)^{1/2} A \\ (f/2)^{1/2} A & \frac{2r^2 + fA^2}{2(f)^{1/2}} \end{pmatrix}, \quad (28)$$

as well as (10)–(11),

$$\partial_r[w + \ln(r^4/f^2)] = \frac{1}{r} \text{Tr}[(\partial_r M)M^{-1}]^2 - ((\partial_z M)M^{-1})^2, \quad (29)$$

$$\partial_z[w + \ln(r^4/f^2)] = \frac{2}{r} \text{Tr}[(\partial_r M)M^{-1}](\partial_z M)M^{-1}. \quad (30)$$

Note that the matrix M is symmetric and $\det(M) = r^2$. Eq. (27) is mathematical equivalent to the Ernst equation, although the physical and geometric content of these equations are different [18]. Now we shall study models of disks based in simple solutions of (27)

A. Disk Associated with a Magnetic Dipole Solution

A Kerr like solution to (27) is

$$f^{1/2} = \frac{p^2x^2 - q^2y^2 - 1}{(px + 1)^2 - q^2y^2}, \quad (31)$$

$$A = -2\sqrt{2}pq \frac{p(x^2 - y^2) + x(1 - y^2)}{p^2x^2 - q^2y^2 - 1}, \quad (32)$$

where x and y are the spheroidal coordinates

$$2px = \sqrt{r^2 + (z + p)^2} + \sqrt{r^2 + (z - p)^2}, \quad (33)$$

$$2py = \sqrt{r^2 + (z + p)^2} - \sqrt{r^2 + (z - p)^2}, \quad (34)$$

p and q are two constants related by

$$q^2 = p^2 - 1. \quad (35)$$

The function w is given by

$$e^w = f^2 F^4, \quad (36)$$

with

$$F = \frac{p^2x^2 - q^2y^2 - 1}{p^2((px + 1)^2 - q^2y^2)}. \quad (37)$$

A similar solution, but in a different system of coordinates, was first studied by Bonnor [23], for $p = 1$ reduces to the Weyl γ -metric (with $\gamma = 2$). This solution can be interpreted as a Weyl γ -metric with a magnetic dipole located in the origin of the coordinate system.

Now we perform the “displace, cut and reflect” method above mentioned, i.e., we do $z \rightarrow z_0 + |z|$ in the Kerr like solution. This is equivalent to change only the definitions of the coordinates x and y by the new definition

$$2px = \sqrt{r^2 + (|z| + z_0 + p)^2} + \sqrt{r^2 + (|z| + z_0 - p)^2}, \quad (38)$$

$$2py = \sqrt{r^2 + (|z| + z_0 + p)^2} - \sqrt{r^2 + (|z| + z_0 - p)^2}. \quad (39)$$

Now, the computation of the physical quantities like σ, p_φ , etc. associated to this disk is straight forward, but the result is rather cumbersome,

$$\begin{aligned} \sigma &= 8[(2\bar{y}z_0 - 3)\bar{x}^2 - \bar{y}^2 - (\bar{x}^2 + \bar{y}^2)p\bar{x}]p^2\bar{y} + (\bar{x}^2 + \bar{y}^2 - 2q^2\bar{x}^2\bar{y}^2)z_0 \\ &\quad + ((3\bar{y}z_0 - 2)\bar{y} + \bar{x}^2z_0 + (\bar{x}^2 + \bar{y}^2)q^2\bar{y})p\bar{x}]p^2 / \\ &\quad [(q^2\bar{y}^2 + 1 - p^2\bar{x}^2)(q\bar{y} + 1 + p\bar{x})^2(q\bar{y} - 1 - p\bar{x})^2], \end{aligned} \quad (40)$$

$$\begin{aligned} p_\varphi &= 8((\bar{x}^2 + \bar{y}^2)q^2 + 2)p\bar{x}\bar{y} - (\bar{x}^2 + \bar{y}^2 + 2q^2\bar{x}^2\bar{y}^2)z_0 - ((\bar{x}^2 + \bar{y}^2)p - \\ &\quad 2\bar{x}\bar{y}z_0)p^2\bar{x}\bar{y}]p^2 / [(q^2\bar{y}^2 + 1 - p^2\bar{x}^2)^2(q\bar{y} + 1 + p\bar{x})(q\bar{y} - 1 - p\bar{x})], \end{aligned} \quad (41)$$

$$\begin{aligned} j_\varphi &= -4\sqrt{2}[((3\bar{y}^2 - 1)\bar{x}^2z_0 + 4\bar{y} + 2(\bar{x}^2 + \bar{y}^2)q^2\bar{y})p\bar{x} - \\ &\quad ((\bar{y}^2 + 2\bar{y}z_0 - 1)\bar{y} - 2(\bar{y} - z_0)\bar{x}^2 + (4\bar{x}^2\bar{y}z_0 - 2\bar{x}^2 + \\ &\quad \bar{y}^4 - \bar{y}^2)q^2\bar{y})]p - ((\bar{y}^2 + 1 - (\bar{y}^2 - 3)q^2\bar{y}^2)z_0 + 2(\bar{x}^2 + \bar{y}^2)p^4\bar{y} \\ &\quad + (\bar{y}^2 - 4\bar{y}z_0 - 1 + 2\bar{x}^2)p^3\bar{x}\bar{y})\bar{x}]q / (\bar{x}^2 - \bar{y}^2)^3, \end{aligned} \quad (42)$$

where

$$2p\bar{x} = \sqrt{r^2 + (z_0 + p)^2} + \sqrt{r^2 + (z_0 - p)^2}, \quad (43)$$

$$2p\bar{y} = \sqrt{r^2 + (z_0 + p)^2} - \sqrt{r^2 + (z_0 - p)^2}. \quad (44)$$

The magnetic potential A is given by the same function (32) but with x and y given by (38) and (39).

We shall study the above functions graphically. In Fig. 2 we present the surface density σ as a function of the radial coordinate r for $z_0 = 2$ and different values of the parameter q that controls the magnetic field.

The density have a finite central maximum that decays fast. The curve with the lowest maximum has $q = 0$ and the next three curves have $q = 0.5, 1$, and 1.5 . The curve with $q = 0$ represents the density of a disk with no magnetic field, i.e., the density of a usual cold disk. We see that the inclusion of the magnetic field increases the central density for the values of q shown. Really, the central density increases up to a value close to 2.5 for $q = 1.73$ and for values of $q \geq 1.73$ decreases very fast and take negative values (not shown in the figure).

The azimuthal pressure is shown in Fig. 3 for $z_0 = 2$ and $q = 0$ (bottom curve), $0.5, 1, 1.5$ (top curve). We have that the pressure has a maximum that increases with q and moves toward the disk centre. For $q \geq 1.5$ we have similar behavior.

The azimuthal current is presented in Fig. 4 for the same values of the parameters z_0 and q . The curve that corresponds to $q = 0$ is the axis r . The

current has similar behavior than the pressure. We see that the behavior of the current and the pressure is consistent with the presence of a ring-like current of massless particles.

In Fig. 5 we present the magnetic potential A and its level curves that represent the the magnetic field for $z_0 = 2$ and $q = 1$. We see that the form of the magnetic field also supports the idea of a ring-like current distribution.

Finally for this disk, we shall examine the stability against radial perturbations (ring formation). In Fig. 6 we present the radial dependence of the angular momentum h for a cold disk $q = 0$ for $z_0 = 2$ (top curve), $z_0 = 2.5, 4, 3.4$ and 4 (bottom curve). We see the the disk with $z_0 = 2$ is unstable, h is not an increasing function of r for $0 \leq r \leq 14$. This is a pure general relativistic instability. Now we shall study the stability of the disk with $z_0 = 2.5$ when we switch on the magnetic field.

The radial dependence of the angular momentum h is presented in Fig. 7 for $q = 0$ (bottom curve), $0.5, 1, 1.5$ (top curve). Therefore the disk with $q = 1.5$ is unstable. Again the magnetic field introduces a pure gravitational instability. Note that the disk with $q = 0$ is stable and the inclusion of the magnetic field makes it gravitationally unstable. The density, pressure and current for this disk look similar than the ones for $z_0 = 2$, we shall comeback to this point later.

B. A disk associated with Taub-NUT like charge

A Taub-NUT like solution is,

$$f^{1/2} = \frac{p^2(x^2 - 1)}{px^2 + 2x + p}, \quad (45)$$

$$A = 2\sqrt{2}by/p, \quad (46)$$

$$F = \frac{px^2 + 2x + p}{p(x^2 - y^2)}, \quad (47)$$

with

$$b^2 = 1 - p^2. \quad (48)$$

The function w is given by (36), b is a constant and x and y are the same coordinates defined before. This solution for $p = 1$ also reduces to the Weyl γ -metric (with $\gamma = 2$).

As in the precedent case we find,

$$\sigma = -8[(\bar{y}^2 + 2 + \bar{x}^2)p^2\bar{y} - (\bar{x}^2 + 3\bar{y}^2)z_0]\bar{x} - ((2\bar{y}^2z_0 - 3\bar{y} +$$

$$z_0\bar{x}^2 - (\bar{y} - z_0)\bar{y}^2)p]/[((\bar{x}^2 + 1)p + 2\bar{x})^2(\bar{x}^2 - 1)p], \quad (49)$$

$$p_\varphi = \frac{-8[((2\bar{y}^2 - 1)\bar{x}^2 - \bar{y}^2)z_0 - (\bar{y}^2 - 2 + \bar{x}^2)p\bar{x}\bar{y}]}{((\bar{x}^2 + 1)p + 2\bar{x})(\bar{x}^2 - 1)^2p}, \quad (50)$$

$$j_\varphi = 4\sqrt{2}(p\bar{x} - \bar{y}z_0)(\bar{x}^2 - 1)^2b/[(\bar{x}^2 - \bar{y}^2)^3p^2]. \quad (51)$$

The magnetic potential A is the given by the same function (46) but with x and y given by (38) and (39).

The surface density as a function of r is presented in Fig. 8 for $b = 0$ (bottom curve), $b = 0.3, 0.6, 0.9$ (top curve) and $z_0 = 2$. We see that the the density maximum increases when the magnetic parameter b increases.

We also see (Fig. 9), for the same value of the parameters, a similar behavior for the current. The curve $b = 0$ is the axis r . The pressure behaves in the opposite way (Fig. 10), it decreases when the magnetic parameter b increases. For the top and bottom curves we have $b = 0$ and $b = 0.9$ respectively.

The field lines of magnetic field in this case are quite simple, they are just parts of hyperbola branches that cut the disk in an axially symmetric way, the axis of the disk being the symmetry axis. Note that the distribution of current is quite different in this case than in the precedent one. Now we have a more homogeneous distribution.

The angular momentum h as a function of r is shown in Fig. 11 for $z_0=2$ and $b = 0$ (top curve), $b = 0.3, 0.6, 0.9$ (bottom curve). We see that the inclusion of the magnetic parameter can stabilize the disk. We shall comeback to this point later.

C. A generalization of a Lynden-Bell-Pinault solution

A magnetized Lynden Bell-Pinault like solution is

$$f^{1/2} = a^2/f_0 + c^2r^2/f_0, \quad (52)$$

$$A = -\sqrt{2}\frac{abf_0 + dcr^2}{a_0^2 + c^2r^2} \quad (53)$$

$$w = w_0 + 2\ln(f/f_0) - 8\ln a, \quad (54)$$

where f_0 and w_0 are the respective functions associated to the Lynden-Bell-Pinault solution [9]:

$$f_0 = [(z + \sqrt{r^2 + z^2})/2]^{2n}, \quad (55)$$

$$w_0 = 4n^2 \ln \frac{z + \sqrt{r^2 + z^2}}{2\sqrt{r^2 + z^2}}, \quad (56)$$

a, b, c, d and n are constants restricted by the relations $ad - cb = \pm 1$, and $n \leq 1$. This solution was found by applying the transformation $M = B^{-1}M_0B$ with

$$B = \begin{pmatrix} a & b \\ c & d \end{pmatrix}. \quad (57)$$

M_0 being the matrix (28) com $A = 0$. Note the right hand side of Eqs. (29) and (30) are invariant under the transformation $M = B^{-1}M_0B$.

Now doing $z \rightarrow |z| + z_0$ in the previous solution we find after doing $z_0 = 0$,

$$\sigma = r^{3n}2^{2n^2-n+2}(1-n)a^4n/[(r^{2n}a^2 + 2^{2n}c^2r^2)r] \quad (58)$$

$$p_\varphi = r^{3n-1}2^{2n^2-n+2} \frac{[r^{2n}a^2n - 2^{2n}(2-n)c^2r^2]a^4n}{(r^{2n}a^2 + 2^{2n}c^2r^2)^2} \quad (59)$$

$$j_\varphi = \pm 2^{2n+5/2-2n^2} cnr^{1-2n}/a^3. \quad (60)$$

Note that this solution has well behave density that is singular in the center of the disk, like the original LBP solution. The pressure is positive in the center, but for $r > r_c$ it becomes negative,

$$r_c = \left[\frac{na^2}{2^{2n}(2-n)c^2} \right]^{1/(2-2n)}, \quad (61)$$

i.e., we have tensions. This is a general feature of solutions generated in the same form using a Weyl solution as a seed.

Hence in this case we have that this particular magnetization of the LBP disk introduces tensions.

D. A particular disk associated to a 1-soliton like solution

A particular 1-soliton solution is

$$f^{1/2} = \frac{(c_0^2 + c_1^2)\mu r}{c_0^2\mu^2 - c_1^2r^2}, \quad (62)$$

$$A = -\sqrt{2} \frac{c_0c_1(\mu^2 + r^2)}{(c_0^2 + c_1^2)\mu}, \quad (63)$$

$$F = \frac{c_0^2\mu^2 - c_1^2r^2}{\sqrt{r(c_0^2 + c_1^2)(\mu^2 + r^2)}}, \quad (64)$$

where

$$\mu = z - z_0 + \sqrt{r^2 + (z - z_0)^2} \quad (65)$$

and c_0, c_1 and z_0 are constants. This solution was obtained by applying the Belinsky-Zhakarov [17] method with a single pole scattering matrix. A similar solution was studied in [24]

As before by doing $z \rightarrow |z|$ we find

$$\sigma = 16(c_0^2 + c_1^2)\mu^2 r^2 / [(c_0\mu + c_1 r)^2 (c_0\mu - c_1 r)^2], \quad (66)$$

$$p_\varphi = 8(\mu^2 - r^2) / [(c_0\mu + c_1 r)(c_0\mu - c_1 r)] \quad (67)$$

$$j_\varphi = 4\sqrt{2}r\mu^2(\mu^2 - r^2)c_0c_1 / (\mu^2 + r^2)^3 \quad (68)$$

For this solution we have that the central density of the disk is zero but not the pressure.

In the four solutions presented we have chosen the integrations constants associated with the quadrature of w in such a way that $w \rightarrow 0$ on the symmetry axis. Thus we have a regular symmetry axis outside the sources. There are many known exact solutions of the Einstein-Maxwell equations with axial symmetry, as well as, many methods to find them. In particular, the first two solutions presented are specializations of a Kerr-NUT like solution or two soliton solution. We have presented them separated because of algebraic simplicity.

4 Discussion

For the disks studied in the present paper we made a rather complete study of parameters, we only mentioned the more relevant aspects of each solution. In particular, for solutions generated from finite sources like the one in Fig. 1, we have that the density of the disk is a decreasing function of the “cut” parameter z_0 . For a Newtonian disk generated from Newton’s law $\Phi \sim M/\sqrt{r^2 + z^2}$ the “displace, cut, and reflect method” gives the surface density $\sigma_N \sim Mz_0/(r^2 + z_0^2)^{3/2}$ (Kusmin-Toomre disk). Thus the central density $\sigma_N(0) \sim M/z_0^2$. For the first two studied disks A. and B. we put the “mass” parameter equal to one. This is equivalent to have coordinates t, r, z dimensionless, one can recuperate this parameter by multiplying the line element by m . The numerical study of the two first disks shows that the central density also decays with z_0 , but with a different law than the Kusmin-Toomre disk.

We find that the magnetic field stabilize the disk against radial perturbation when the distribution of current that generate the field has its origin in a NUT like parameter. And made the disk unstable when the distribution of current is originated by a Kerr like parameter. In a different, context we studied a similar phenomena, we found that the inclusion of magnetic mass in a Weyl solution with unstable orbits (Schwarzschild solution plus a dipolar halo) makes the orbits less chaotic [25], i.e., more stable. Also the opposite is true for particles moving in counter rotation in a slow rotating Kerr solution plus a dipolar halo. The rotation makes the orbits more chaotic [26]. These are pure general relativistic effects.

In the present work we studied simple four solutions of the Einstein-Maxwell equation generated by well known new-solution-generating algorithms [18]. There are quite a few solutions of the Einstein Maxwell equations with axial symmetry that can be used to generate disks. For instance in the present context members of a Tomimatsu-Sato like family of solutions are good candidates. But the algebraic complexity involved in the finding of the physical variables of the disks is not trivial.

The hot disks studied in this paper have not radial pressure nor the charges have mass. There are several methods to add radial pressure to disks, they are based in the fact that a coordinate transformation that keep $detM$ as a harmonic function in the variables r, z does not change the form of the metric (1).

A second degree of complexity is to add rotation to the disks, also suitable solutions of the Einstein-Maxwell equations for stationary spacetimes are well known. Again the algebraic complexity is not trivial in this case. The inclusion of rotations, in principle, can be used to introduce mass in the charge carriers. A particular case of hot rotating disk is under study.

Finally, we want to mention that all the computation of this work was performed using the algebraic programming system Reduce [27]

Acknowledgments

I want to thank CNPq and FAPESP for financial support. Also S.R. Oliveira for discussions.

References

- [1] S.L. Shapiro and S.A. Teukolsky, “Black Holes, White Dwarfs, and Neutron Stars” (J. Wiley, New York 1983). Chapter 7
- [2] S.S. Balbus and J.F. Hawley, *Rev. Mod. Phys.* 70, 1 (1998)
- [3] W. A. Bonnor and A. Sackfield, *Comm. Math. Phys.* 8, 338 (1968)
- [4] T. Morgan and L. Morgan, *Phys. Rev.* 183, 1097 (1969)
- [5] L. Morgan and T. Morgan, *Phys. Rev. D*2, 2756 (1970)
- [6] A. Chamorro, R. Gregory and J. M. Stewart, *Proc. R. Soc. Lond.* A413, 251 (1987)
- [7] G. González and P.S. Letelier *Class. Quan. Grav.* 16, 479 (1999)
- [8] P. S. Letelier and S. R. Oliveira, *J. Math. Phys.* 28, 165 (1987)
- [9] D. Lynden-Bell and S. Pineault, *Mon. Not. R. Astron. Soc.* 185, 679 (1978)
- [10] J. P. S. Lemos, *Class. Quan. Grav.* 6, 1219 (1989)
- [11] J. P. S. Lemos and P. S. Letelier, *Class. Quan. Grav.* 10, L75 (1993)
- [12] J. P. S. Lemos and P. S. Letelier, *Phys. Rev D*49, 5135 (1994)
- [13] J. P. S. Lemos and P. S. Letelier, *Int. J. Mod. Phys. D*5, 53 (1996)
- [14] C. Klein, *Class. Quan. Grav.* 14, 2267 (1997)
- [15] J. Bičák, D. Lynden-Bell and J. Katz, *Phys. Rev. D*47, 4334 (1993)
- [16] J. Bičák, D. Lynden-Bell and C. Pichon, *Mon. Not. R. Astron. Soc.* 265, 126 (1993) 280, 1007 (1996)
- [17] V.A. Belinsky and V. Zakharov, *Sov. Phys. JEPT* 50, 1 (1979) [*Zh. Eksp. Teor. Fiz.* 77, 3 (1979)]
- [18] D. Kramer, H. Stephani, M. McCallum and E. Herlt. *Exact Solutions of Einstein’s Field Equations*. Cambridge University Press, Cambridge (1980)
- [19] G. Kusmin, *Astron. Zh.*, 33, 27 (1956)

- [20] A. Toomre, Ap. J. 138, 385 (1962)
- [21] L.D. Landau and E.M. Lifshitz, “ Fluid Mechanics” (Addison-Wesley, Reading 1989), Chapter 3.
- [22] R. Geroch, J. Math. Phys. 12, 918 (1971); 13, 394 (1972)
- [23] W.B. Bonnor, Z. Phys. 190, 444 (1966)
- [24] P.S. Letelier, J. Math. Phys. **26**, 467 (1985)
- [25] P.S. Letelier and W.M. Vieira, Phys. Letts A244, 324 (1998).
- [26] P.S. Letelier and W.M. Vieira, Phys. Rev. D 56, 8095-8098 (1997).
- [27] A.D. Hearn and J.P. Fitch, REDUCE User’s Manual (Konrad-Zuse-Zentrum, Berlin 1998)

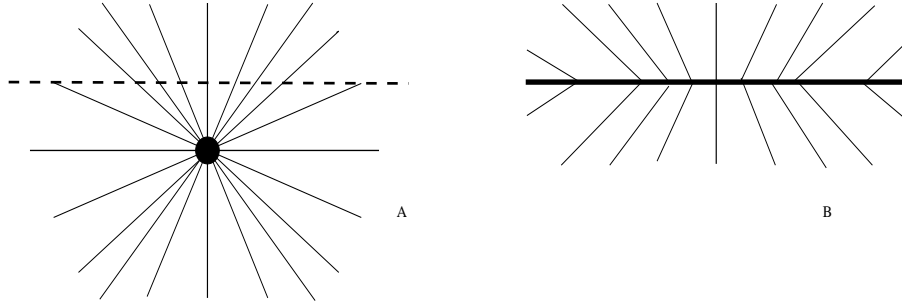


Fig. 1. The illustration of the “displace, cut, and reflect” method for the generation of a disk from the gravitational field of a punctual mass. In A we displace and cut out the singularity with a plane, in B we reflect the field on the plan. We end up with the field of a disk.

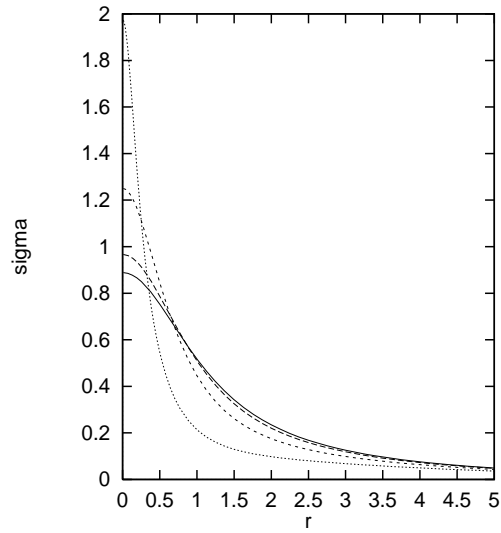


Fig. 2. The surface density σ as a function of r for $z_0 = 2$ for $q = 0$ (lower maximum), 0.5, 1, 1.5 (higher maximum). The parameter q controls the magnetic field.

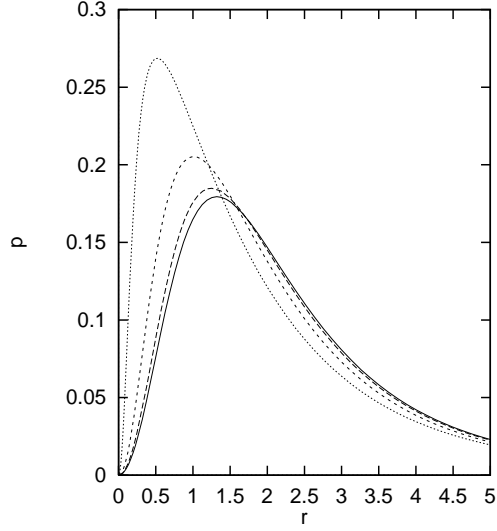


Fig. 3. The azimuthal pressure for $z_0 = 2$ and $q = 0$ (bottom curve), 0.5, 1, 1.5 (top curve). We have that the pressure has a maximum that increases with q and moves toward the disk centre.

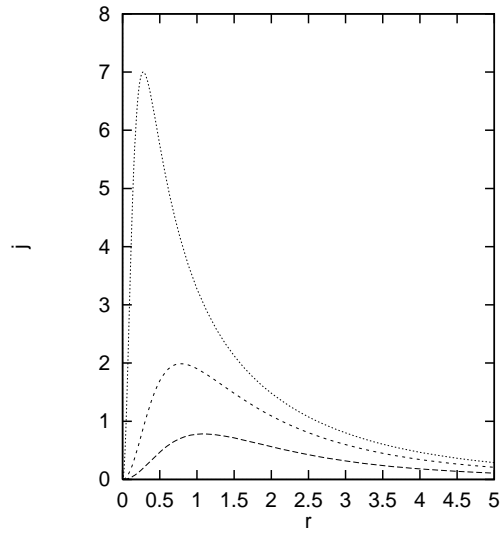


Fig. 4. The azimuthal current for the same values of the parameters z_0 and q . The curve that corresponds to $q = 0$ is the axis r .

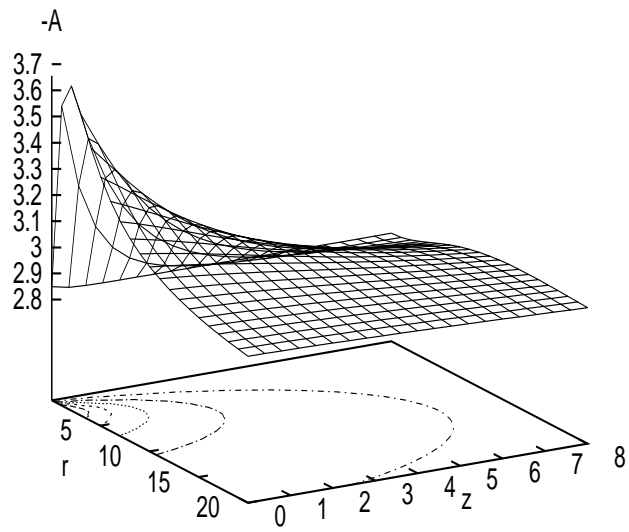


Fig. 5. The function A and its level curves that represent the the magnetic field for $z_0 = 2$ and $q = 1$. We see that the form of the magnetic field support the idea of a ring-like current distribution.

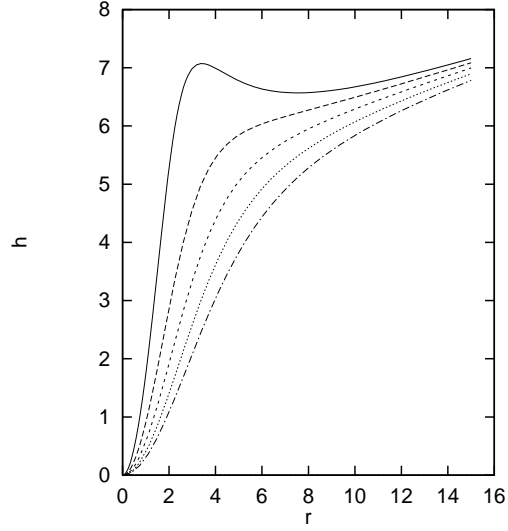


Fig. 6. The radial dependence of the angular momentum h for a cold disk $q = 0$ for $z_0 = 2$ (top curve), $z_0 = 2.5, 4, 3.4$ and 4 (bottom curve).

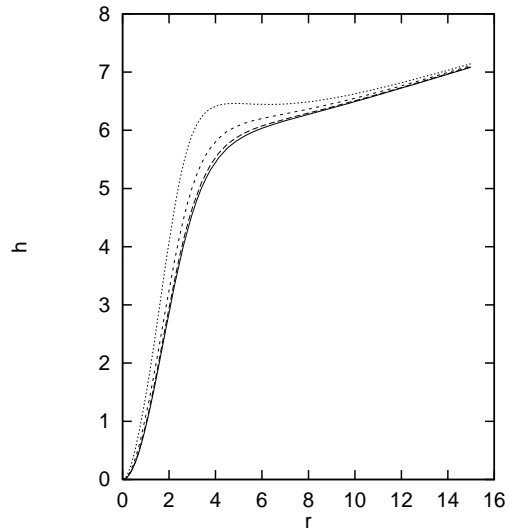


Fig. 7. The radial dependence of the angular momentum h for $q = 0$ (bottom curve), $0.5, 1, 1.5$ (top curve). In this case colder disks are more stable.

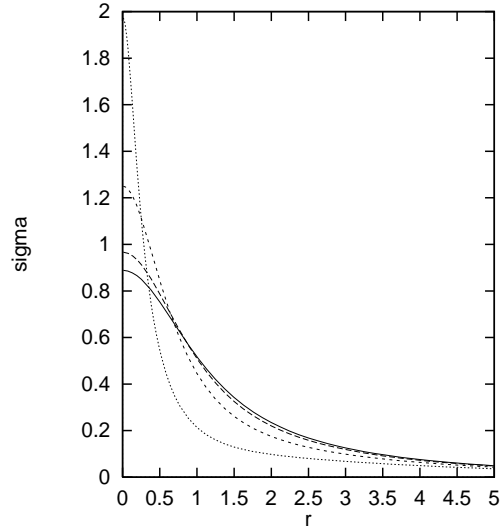


Fig. 8. The surface density as a function of r for $b = 0$ (bottom curve), $b = 0.3, 0.6, 0.9$ (top curve) and $z_0 = 2$. The density maximum increases when the magnetic parameter b increases.

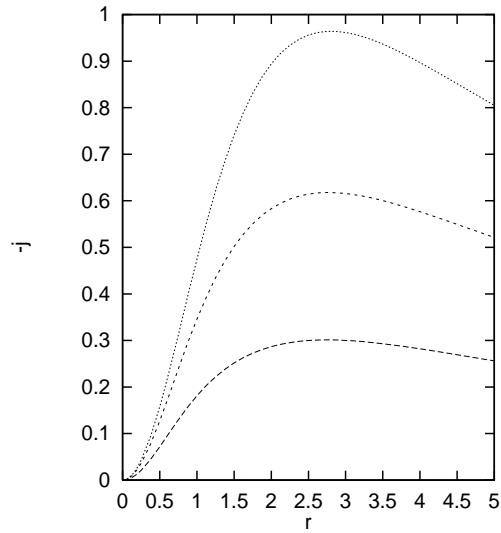


Fig. 9. The current for the same value of the parameters of Fig 8. The curve $b = 0$ is the axis r . The current and the density have a similar behavior.

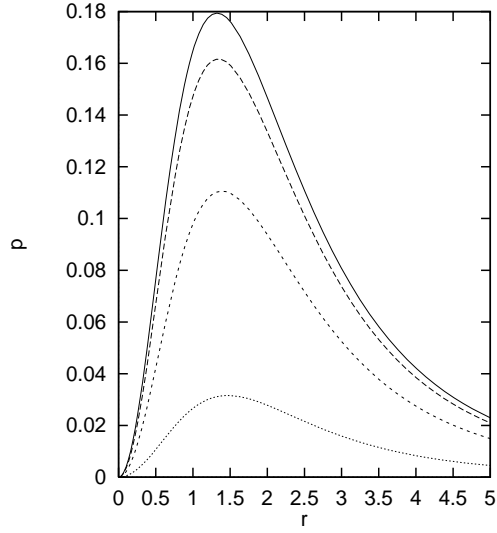


Fig 10. The pressure decreases when the magnetic parameter b increases. For the top and bottom curves we have $b = 0$ and $b = 0.9$, respectively.

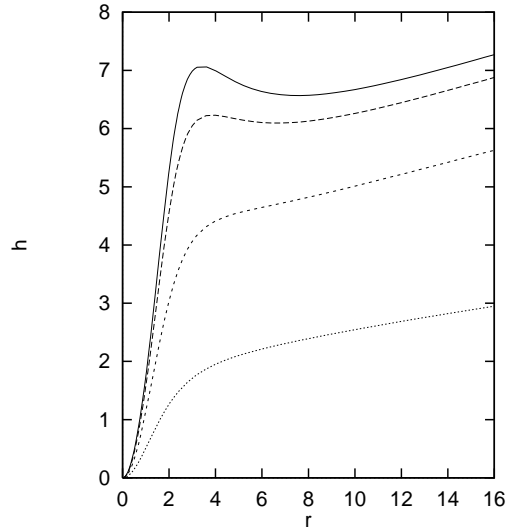


Fig. 11. h as a function of r for $z_0=2$ and $b = 0$ (top curve), $b = 0.3, 0.6, 0.9$ (bottom curve). In this case hotter disks are more stable.